

---

This is an electronic reprint of the original article.  
This reprint may differ from the original in pagination and typographic detail.

Borrega, Marc; Larsson, Per Tomas; Ahvenainen, Patrik; Ceccherini, Sara; Maloney, Thaddeus; Rautkari, Lauri; Sixta, Herbert

**Birch wood pre-hydrolysis vs pulp post-hydrolysis for the production of xylan-based compounds and cellulose for viscose application**

*Published in:*  
Carbohydrate Polymers

*DOI:*  
[10.1016/j.carbpol.2018.02.064](https://doi.org/10.1016/j.carbpol.2018.02.064)

Published: 15/06/2018

*Document Version*  
Peer-reviewed accepted author manuscript, also known as Final accepted manuscript or Post-print

*Published under the following license:*  
CC BY-NC-ND

*Please cite the original version:*  
Borrega, M., Larsson, P. T., Ahvenainen, P., Ceccherini, S., Maloney, T., Rautkari, L., & Sixta, H. (2018). Birch wood pre-hydrolysis vs pulp post-hydrolysis for the production of xylan-based compounds and cellulose for viscose application. *Carbohydrate Polymers*, 190, 212-221. <https://doi.org/10.1016/j.carbpol.2018.02.064>

# Birch wood pre-hydrolysis vs pulp post-hydrolysis for the production of xylan-based compounds and cellulose for viscose application

Marc Borrega<sup>a,b\*</sup>, Per Tomas Larsson<sup>c</sup>, Patrik Ahvenainen<sup>d</sup>, Sara Ceccherini<sup>a</sup>, Thaddeus Maloney<sup>a</sup>, Lauri Rautkari<sup>a</sup>, Herbert Sixta<sup>a</sup>

<sup>a</sup> *Department of Bioproducts and Biosystems, Aalto University, PO BOX 16300, 00076 Aalto, Finland*

<sup>b</sup> *VTT Technical Research Centre of Finland Ltd, PO BOX 1000, 02044 VTT, Finland*

<sup>c</sup> *RISE Bioeconomy, PO Box 5604, 11486 Stockholm, Sweden*

<sup>d</sup> *Department of Physics, University of Helsinki, PO Box 64, 00014 Helsinki, Finland*

## Abstract

Hydrothermal treatments of birch wood and kraft pulp were compared for their ability to extract the xylan and produce viscose-grade pulp. Water post-hydrolysis of kraft pulp produced a high-purity cellulosic pulp with lower viscosity but higher cellulose yield than traditional pre-hydrolysis kraft pulping of wood. Post-hydrolysis of pulp also increased the crystallite dimensions and degree of crystallinity in cellulose, and promoted a higher extent of fibril aggregation. The lower specific surface area in post-hydrolyzed pulps, derived from their larger fibril aggregates, decreased the accessibility of -OH groups. However, this lower accessibility did not seem to decrease the pulp reactivity to derivatizing chemicals. In the aqueous side-stream, the xylose yield was similar in both pre- and post-hydrolysates, although conducting post-hydrolysis of pulp in a flow-through system enabled the recovery of high purity and molar mass (~10 kDa) xylan for high-value applications.

## Keywords:

Cellulose, dissolving pulp, hydrothermal treatment, viscose, xylan

\*Corresponding author

Present address:

Marc Borrega

VTT Technical Research Centre of Finland Ltd.

PO Box 1000, FI-02044 VTT, Finland

+358 40482 0837

[marc.borrega@vtt.fi](mailto:marc.borrega@vtt.fi)

## 1. Introduction

In the last decade, the wood pulping industry has experienced a steady increase in the demand of dissolving-grade pulps as the world consumption has increased from 3.3 million tons in 2007 to 6.5 million tons in 2015 (FAO Yearbook 2007, 2015). Dissolving pulps, containing over 90% cellulose and low amounts of impurities, are used in the manufacture of regenerated cellulose fibers, cellulose ethers, and cellulose esters for a wide range of applications, i.e., textiles, films, food, drugs. The high demand for dissolving pulps, mostly driven by the production of viscose fibers for textiles, is partly related to the growing world population and the increasing purchasing power in Asian markets, and thus is expected to continue increasing in the future (Liu, Shi, Cheng, & He, 2016).

Dissolving wood pulps are industrially produced by acid sulfite pulping or by pre-hydrolysis kraft (PHK) pulping. Since both of these processes were developed in the first half of last century, new pulping methods that are in line with the requirements of modern pulp mills are currently being investigated. Such requirements include a higher efficiency in the use of raw materials, lower consumption of chemicals and improved recovery cycle, and diverse product portfolio through valorization of side-streams. Examples of recently developed pulping methods to produce dissolving wood pulps are the SO<sub>2</sub>-ethanol-water pulping (Iakovlev, You, van Heiningen, & Sixta, 2014), and Organosolv-type fractionation processes that utilize organic solvents like  $\gamma$ -valerolactone (Alonso et al., 2017; Lê, Ma, Borrega, & Sixta, 2016) or methyl isobutyl ketone (Bozell et al., 2011). Alternatively, the upgrade of paper (kraft) pulps into dissolving pulps by selectively removing the hemicellulosic fraction is being investigated. Pulp post-treatments are mainly based on the application of enzymatic hydrolysis and cold caustic extraction (Gehmayr, Schild, & Sixta, 2011; Ibarra, Köpcke, & Ek, 2009), nitren extraction (Janzon, Puls, & Saake, 2006), and ionic liquid extraction (Froschauer et al., 2013; Roselli, Hummel, Monshizadeh, Maloney, & Sixta, 2014).

Recently, we have shown that high-purity cellulosic pulp can also be produced by water post-hydrolysis of hardwood kraft pulp (Borrega & Sixta, 2013; Borrega, Concha-Carrasco, Pranovich, & Sixta, 2017), in which the water hydrolytic stage is implemented after pulping, instead of prior to pulping as in a conventional PHK process. Water post-hydrolysis of pulp requires elevated temperatures around 240 °C, but the treatment times are very short ( $\leq 10$  min). One of the main benefits of water post-hydrolysis, compared to other pulp post-treatments reported in the literature, is that water is the only solvent used, and thus complex and costly chemical recovery systems are not required. The pulp quality, in terms of chemical and macromolecular properties, appears to be comparable to that of commercial PHK pulps for viscose application (Borrega et al., 2017). Nonetheless, the most important quality parameter of any dissolving pulp is probably its so-called reactivity.

Pulp reactivity refers to the tendency of the pulp to react with derivatising chemicals under certain reaction conditions. The pulp reactivity is a function of its chemical, molecular and fibrillar features, and thus cannot be defined by a single parameter (Sixta, 2006). In practice, however, the chemical reactivity of pulp is typically estimated with indirect methods that determine its solubility in a specific solvent system. In the viscose industry, the most reliable indicator to assess the pulp reactivity is the filterability value of the cellulose xanthate as determined by the Treiber test, which mimics all the steps applied in the actual conversion of pulp into viscose dope. This method is not only complex and time-consuming, but also needs special equipment and relatively large amounts of pulp material, making the analyses difficult in laboratory scale. Therefore, the Fock test, a simplified method that quantifies the amount of cellulose dissolved (or regenerated) in a solution containing sodium

hydroxide (NaOH) and carbon disulfide (CS<sub>2</sub>), is commonly used to provide a measure of the pulp reactivity in viscose conversion (Christoffersson, Sjöström, Edlund, Lindgren, & Dolk, 2002; Engström, Ek, & Henriksson, 2006; Miao et al., 2014). Since the reactivity is related to the accessibility of functional groups in the pulp, predominantly hydroxyl groups (-OH), it may also be estimated from several molecular and structural features (Gehmayr et al., 2011; Wollboldt, Zuckerstätter, Weber, Larsson, & Sixta, 2010). In this article, we will discuss the pulp reactivity based on its solubility behavior in chemical solvent systems.

In recent years, the transformation of traditional pulp mills into advanced biorefineries, having a wider product portfolio than simply paper- or dissolving-grade pulp, has attracted a lot of attention. Modern pulp mills (biorefineries) are regarded as one of the cornerstones for the development of biobased economies. Within this context, water post-hydrolysis of pulp is of interest because, if applied in a flow-through system, the extracted hemicelluloses may be recovered from the aqueous hydrolysate in high yield and relatively high molar mass, depending on the flow rate (Borrega & Sixta, 2013; Borrega, Concha-Carrasco, Pranovich, & Sixta, 2017). Hemicelluloses are valuable sugars that can be utilized in a wide range of chemical and material applications (Deutschmann & Dekker, 2012; Hansen & Plackett, 2008). It should be mentioned that the extraction and recovery of hemicelluloses for their subsequent valorization can also be realized by water pre-hydrolysis of wood. However, the presence of other chemical compounds originating from lignin and extractives in the wood pre-hydrolysates tends to complicate the recovery of hemicelluloses using membrane separation techniques (Koivula et al., 2011). Owing to the more homogenous composition of pulp, compared to wood, the recovery of the hemicelluloses from post-hydrolysates may be accomplished rather easily by membrane ultrafiltration.

In this study, we have compared the performance of pre- and post-hydrolysis processes to produce viscose-grade pulp on the one hand, and xylan-based sugars on the other hand. Water pre-hydrolysis experiments of birch wood under different intensities were first conducted prior to kraft pulping. After pulping, the unbleached pulps were subjected to post-hydrolysis experiments to further decrease the xylan content, and selected pulps with potential to be used in viscose production were then bleached. The chemical, molecular, and supramolecular properties of the bleached pulps were thoroughly characterized and related to the accessibility and reactivity of the pulps. Finally, the recovery of sugars from the aqueous hydrolysates as well their chemical and molecular characteristics were determined. Based on the results, the advantages and disadvantages of water pre- and post-hydrolysis processes are here presented.

## **2. Experimental**

### *2.1. Wood material*

Birch (*Betula spp.*) wood chips were delivered by a pulp mill in Finland. Upon delivery, the chips were screened according to the SCAN-CM 40:01 method and stored in the freezer until further use. The identified chemical composition of the wood was 38.4% glucose, 20.8% xylose, 1.6% mannose, 0.6% galactose, 0.4% rhamnose, 0.3% arabinose, 20.7% acid insoluble (Klason) lignin and 4.8 % acid soluble lignin (ASL).

### *2.2. Production of pulps*

A series of pulps were produced by water pre-hydrolysis, kraft pulping, and water post-hydrolysis. Pre-hydrolysis of birch wood chips was conducted in 2.5 L autoclaves in a rotating air-bath digester (Haato Oy, Finland), at a liquid-to-wood ratio of 4:1 L/kg. The temperature in the autoclaves was raised to 170 °C and kept constant until

a predetermined P-factor (170, 550, or 1000) was reached. The P-factor is an intensity factor that combines the effects of temperature and time into a single variable, using an Arrhenius-type equation with an activation energy of 125.6 kJ mol<sup>-1</sup>, corresponding to the removal of easily degradable xylan (Sixta, 2006). Once the P-factor was reached, the autoclaves were submerged in a cold water-bath to quench further reactions. The aqueous hydrolysate and pre-hydrolyzed chips were separated by filtration and stored for subsequent experiments and analyses. About 8-10 grams (o.d.) of chips from each pre-hydrolysis experiment, roughly corresponding to 5% of the initial mass of wood charged into the autoclave, were oven-dried, thoroughly washed, and oven-dried again to determine the wood yields after washing.

Kraft pulping of raw and pre-hydrolyzed wood chips (without washing) was conducted in the air-bath digester at a liquid-to-wood ratio of 4:1 L/kg. White liquor was prepared from concentrated solutions of NaOH and Na<sub>2</sub>S in deionized water. The effective alkali (EA) charge was 19% on initial oven-dry (o.d.) wood, and the sulphidity was 30%. The temperature in the autoclaves was raised to 155 °C and kept constant until a predetermined H-factor (200, 400, 650, or 1000) was reached. Similar to the P-factor, the H-factor is an intensity factor that combines the effects of pulping temperature and time into a single variable (Vroom, 1957). The H-factor was selected in order to reach a kappa number of about 16 in the unbleached pulp. The pulping was ended by submerging the autoclaves in a cold water-bath, and after cooling, the pulp was recovered by filtration, thoroughly washed, and screened in a table-top plate screener (0.35 mm mesh). The amount of rejects was less than 0.5% on dry pulp.

Water post-hydrolysis of unbleached kraft and PHK pulps was conducted in a 190 mL flow-through percolation reactor (Unipress Equipment, Poland). About 15 g (o.d.) of pulp were placed in the reactor, equipped with a high-pressure pump, preheater and electric heaters, heat exchanger, and back-pressure regulator (BPR). Water at room temperature was initially pumped through the reactor to wet the pulp and to set the BPR to the operating pressure. The preheater was then turned on, and once the water reached the desired setup temperature, the hot water was circulated into the reactor. The aqueous hydrolysate exiting the reactor was immediately cooled by the heat exchanger and collected in a sampling container. After a predetermined amount of time, the pump was stopped and the pulp was washed (and cooled) by circulating cold tap water through the reactor. The treatment temperature was 240 °C, treatment times ranged from 3 to 15 min, and the flow rate was 400 mL/min.

Selected pulps were bleached following a D<sub>0</sub>-Ep-P sequence. The bleaching conditions were: D<sub>0</sub>: temperature 50 °C, 60 min, kappa factor 0.25; Ep: temperature 70 °C, 60 min, 1.5% NaOH, 0.5% H<sub>2</sub>O<sub>2</sub>; P: temperature 70 °C, 120 min, 0.6% NaOH, 0.5% H<sub>2</sub>O<sub>2</sub>, 0.5 kg of Mg per ton of o.d. pulp. The pulp consistency was 10% in all bleaching stages, and the bleaching was performed in plastic bags heated by steam in a water-bath. Bleaching yields were not determined.

### 2.3. Chemical composition

The carbohydrates and lignin composition in wood and pulp was determined after a two-stage acid hydrolysis, according to the analytical method NREL/TP-510-42618 issued by the US National Renewable Laboratory (NREL). Neutral monosaccharides were determined by high-performance anion exchange chromatography with pulse amperometric detection (HPAEC-PAD) in a Dionex ICS-3000 (Sunnyvale CA, USA) system, equipped with a CarboPac<sup>TM</sup> PA-20 (3.0 X 150 mm) analytical column. Milli-Q water was the eluent used, with a flow rate of 0.4 mL/min at 30 °C temperature. Based on the amount of neutral monosaccharides, the cellulose, xylan and glucomannan fractions in the lignocellulosic material were calculated with the Janson's formulas (Janson, 1970).

With these formulas, cellulose is defined as the content of anhydroglucose in the sample after subtracting the contribution of glucose to glucomannan, and xylan is defined as the content of anhydroxylose and uronic acid constituents. The amount of Klason lignin was quantified gravimetrically, and the amount of ASL was determined in a Shimadzu (Kyoto, Japan) UV-2550 spectrophotometer at a wavelength of 205 nm, using an adsorption coefficient of 110 L/(g·cm). The kappa number in the unbleached pulps was determined according to the SCAN-C 1:100 method.

The chemical composition of aqueous pre- and post-hydrolysates was determined according to the analytical method NREL/TP-510-42623 issued by the US NREL. Monosaccharides were quantified by HPAEC-PAD by direct injection and after total hydrolysis in an autoclave at 121 °C for 60 min. The amount of oligo- and/or polysaccharides was calculated by difference in the monosaccharide content before and after total hydrolysis. The amount of soluble lignin in the hydrolysates was determined in the Shimadzu UV-2550 spectrophotometer at a wavelength of 205 nm, using an adsorption coefficient of 110 L/(g·cm).

#### *2.4. Macromolecular properties*

The intrinsic viscosity of the pulps was determined in 0.5 M cupriethylenediamine (CED) according to the SCAN-CM 15:99 method. Detailed information on the macromolecular properties of bleached pulps was provided by gel permeation chromatography (GPC). For the GPC analyses, the pulps were first activated by a sequential addition of water, acetone, and N,N-dimethylacetamide (DMAc). The activated samples were then dissolved in 90 g/L lithium chloride (LiCl) containing DMAc at room temperature and under gentle stirring. The dissolved samples were diluted to 9 g/L LiCl/DMAc, filtered through 0.2 µm syringe filters, and analyzed in a Dionex Ultimate 3000 (Sunnyvale CA, USA) system, equipped with a guard and four analytical Agilent (Santa Clara, USA) PL-gel Mixed-A columns (7.5 X 300 mm), and coupled with a Shodex (Tokyo, Japan) RI-101 refractive index detector. The flow rate was 0.75 mL/min, and the temperature was 25 °C. Narrow pullulan standards (343 Da - 2350 kDa; PSS, Mainz, Germany) were used to calibrate the system. The molar masses of the pullulan standards were modified to correspond to those of cellulose, as reported in Borrega, Tolonen, Bardot, Testova, & Sixta (2013).

The molar mass characteristics in selected aqueous pre- and post-hydrolysates were determined by size exclusion chromatography (SEC) in a PSS (Mainz, Germany) instrument, equipped with MCX 1000 and 100 000 columns with a pre-column, and coupled with a Waters (Milford, USA) 2414 refractive index detector. Prior to the analyses, the samples were dissolved in 1 M NaOH and filtered through 0.45 µm filters. The SEC measurements were performed in 0.1 M NaOH as eluent, at pH 13, and with a flow rate of 0.5 mL/min at 25 °C temperature. The molar mass distribution (MMD) of the dissolved compounds were calculated against 8 pullulan standards (6.1 - 708 kDa), using the Waters Empower 3 software.

#### *2.5. Supramolecular structure*

Structural characterization of the bleached pulps was performed by cross-polarization magic angle spinning carbon-13 nuclear magnetic resonance (CP/MAS <sup>13</sup>C-NMR) and by wide-angle X-ray scattering (WAXS). For the CP/MAS <sup>13</sup>C-NMR analyses, the pulp samples (water content > 40%) were packed uniformly in a zirconium oxide rotor. The NMR spectra were recorded in a Bruker Avance III AQS 400 SB instrument operating at 9.4 T. All measurements were carried out at 295 (±1) K with a magic angle spinning (MAS) rate of 10 kHz. A 4-mm double air-bearing probe was used. Data acquisition was performed using a cross-polarization (CP) pulse

sequence, i.e., a 2.95 microseconds proton 90-degree pulse and an 800 microseconds ramped (100–50 %) falling contact pulse, with a 2.5 s delay between repetitions. A SPINAL64 pulse sequence was used for  $^1\text{H}$  decoupling. The Hartmann-Hahn matching procedure was based on glycine. The chemical shift scale was calibrated to the TMS-scale (tetramethylsilane,  $(\text{CH}_3)_4\text{Si}$ ) by assigning the data point of maximum intensity in the alpha-glycine carbonyl signal to a shift of 176.03 ppm. Four thousand ninety-six transients were recorded on each sample leading to an acquisition time of about 3 h. The software for spectral fitting was developed at Innventia AB and is based on a Levenberg-Marquardt algorithm (Larsson, Wickholm, & Iversen, 1997). All computations were based on integrated signal intensities obtained from spectral fitting (Wickholm, Larsson, & Iversen, 1998). The errors given for parameters obtained from the fitting procedure are the standard error of the mean with respect to the quality of the fit.

For the WAXS analyses, the pulps (air-dried) were hand-pressed into 2.1 mm thick metal rings and sealed with 6  $\mu\text{m}$  thick Mylar foils. The analyses were performed in a custom-built scattering instrument, consisting of an X-ray generator (Siemens), an X-ray tube with a Cu anode ( $\lambda=1.541 \text{ \AA}$ ) and point focus, a collimating Montel multilayer monochromator, and a two-dimensional image plate detector (MAR345, Marresearch GmbH). A 20-min measuring time was used to record a two-dimensional powder scattering pattern that was averaged over the azimuthal angles to obtain the intensity as a function of the scattering angle (Copper  $\text{K}\alpha$  energy, 8.0 keV). The data were corrected for the noise of the detector, and normalised with the primary beam transmission before Mylar and air background subtraction. Flat panel, polarization and angle-dependent absorption corrections were then applied to the data. The sample crystallinity was estimated by fitting an amorphous background and the 15 strongest reflection of cellulose  $I\beta$  (Nishiyama, Langan, & Chanzy, 2002) to the measured intensities, using the amorphous fitting method presented in Ahvenainen, Kontro, & Svedström (2016). The Gaussian peak fits were used to estimate the average crystallite size based on the 110,  $1\bar{1}0$  and 200 reflections using the Scherrer equation with  $K=0.9$ .

## 2.6. Accessibility by dynamic vapor sorption

The accessible -OH groups in the pulps were quantified after deuteration in a dynamic vapor sorption (DVS) apparatus (Surface Measurement Systems, UK). About 10 mg of air-dry bleached pulp were placed in a small aluminum pan in a climate-controlled chamber of 100  $\text{cm}^3$  volume. The pan was connected to a microbalance with a measuring accuracy of 0.1  $\mu\text{g}$ . The pulp was first dried at 25  $^\circ\text{C}$  by lowering the relative humidity (RH) in the chamber down to 0% with nitrogen gas (flow rate 200  $\text{cm}^3 \text{ min}^{-1}$ ), until the change in pulp mass over a 10-minute period ( $\text{dm}/\text{dt}$ ) was less than 0.0005 %. Thereafter, the RH in the chamber was increased to 95% in a deuterium oxide ( $\text{D}_2\text{O}$ ) atmosphere and kept constant for 10 hours, during which the pulp mass reached an equilibrium. Finally, the RH was lowered again to 0% with dry nitrogen gas until the change in pulp mass over a 10-minute period ( $\text{dm}/\text{dt}$ ) was less than 0.0005 %. Because of the relative difference in molar mass between hydrogen and deuterium, the amount of accessible -OH groups in the pulp sample was calculated according to Eq. 1:

$$A = \frac{m_f - m_i}{m_i} \times 1000 \left( \frac{\text{mmol}}{\text{g}} \right) \quad [1]$$

where A is the amount of accessible -OH groups,  $m_f$  is the dry mass of the deuterated pulp sample at the end of the experiment, and  $m_i$  is the dry mass of pulp after the first drying sequence (before exposure to  $\text{D}_2\text{O}$ ). The atomic

mass difference between deuterium ( $^2\text{H}$ ) and protium ( $^1\text{H}$ ) was approximated to  $1 \text{ g mol}^{-1}$ . Based on the amount of accessible -OH groups and the chemical composition of the pulp, the relative accessibility of -OH groups was calculated from the theoretical value of 18.5 mmol and 15.2 mmol of -OH groups per gram of anhydroglucose (AGU) and anhydroxylose (AXY) units, respectively. It was considered that -OH groups in the C2, C3 and C6 of the AGU unit and those in the C2 and C3 of the AXY unit were accessible.

To exclude any hysteresis effects during the drying-rewetting-drying cycle, two pulp samples containing the highest and lowest amount of hemicelluloses were subjected to the same sorption cycle as described above, but the rewetting stage was performed in a water vapor atmosphere, instead of a  $\text{D}_2\text{O}$  atmosphere. In both samples, the difference in dry mass of pulp between the first and second drying sequence was less than 0.1%.

## *2.7. Reactivity of pulps*

The reactivity of the pulps in a viscose conversion process was estimated by the Fock method; the analyses were performed at MoRe Research (Sweden). With this method, about 0.5 grams of pulp are mixed together with a solution containing sodium hydroxide (NaOH) and excess amounts of carbon disulfide ( $\text{CS}_2$ ) to form cellulose xanthate. By addition of sulfuric acid ( $\text{H}_2\text{SO}_4$ ), some of the cellulose in the xanthate is regenerated, and the yield of regenerated cellulose is given to express the Fock reactivity. In the analyses of our pulps, the concentration of NaOH was 9%, but other experimental details were not disclosed. More information about the principle and details of the Fock method can be found elsewhere (Engström et al., 2006; Tian et al., 2013).

The chemical reactivity of the pulps was further determined by the dissolution-based torque reactivity (DTR) test (Ceccherini & Maloney, 2017). Such test monitors the rheological behavior of pulp fibers during dissolution in CED, and estimates pulp reactivity in terms of dissolution rate and time. Prior to the dissolution tests, the pulps were stored overnight at a solids content of ca. 20%. For each measurement, 0.1875 g (oven dry basis) of pulp were diluted with deionized water to a final solids content of 1.5%. The sample was then placed in a Physica MCR 300 rheometer (Anton Paar GmbH) equipped with 4-blades-vane and basket geometry. The vane height was set at 0.5 mm from the basket bottom, and the temperature was adjusted to  $23^\circ\text{C}$ . The fiber suspension was stirred for an interval of 5 min at  $200 \text{ s}^{-1}$  shear rate, after which the dissolution was started by injecting 12.5 ml of 1 M CED (Sigma Aldrich). While maintaining a constant shear rate, the dissolution of the fibers was monitored by tracking the evolution of torque. The resulting torque vs time rheogram was typically characterized by four consecutive phases: an initial drop, a short linear increase, a nonlinear increase, and a final plateau. The beginning of the plateau corresponded to the completion of the dissolution process. The pulp reactivity was determined by the initial dissolution rate (IDR) and the overall dissolution time ( $\text{T}_{0.1}$ ). The IDR was measured from the linear torque increase, while  $\text{T}_{0.1}$  was the time corresponding to a torque/time ratio of 0.1. This value approximated the beginning of the plateau. High IDR and short  $\text{T}_{0.1}$  values indicated high pulp reactivity.

## **3. Results and discussion**

### *3.1. Yields, chemical composition and macromolecular properties*

The yield of birch wood chips after water pre-hydrolysis decreased along with increasing the P-factor (Table 1). The decrease in wood yield was mainly caused by the removal of the hemicelluloses (predominantly xylan), since the cellulose and lignin yields remained rather similar under the present pre-hydrolysis intensities (supplementary material). This was in agreement with numerous studies dealing with the effects of water pre-hydrolysis on the



chemical composition of various woods (Borrega, Tolonen, Bardot, Testova, & Sixta, 2013; Liu, Li, Luo, Chen, & Huang, 2015; Song, Pranovich, Summerskiy, & Holmbom, 2008; Testova, Chong, Tenkanen, & Sixta, 2011). After kraft pulping, the pulp yield decreased even further (Table 1), due to the concomitant removal of lignin and carbohydrates from the fiber cell wall. The cellulose yield after pulping decreased with increasing pre-hydrolysis intensity (supplementary material), probably due to peeling reactions in alkaline media, following the cleavage of glycosidic bonds in cellulose during pre-hydrolysis and the consequent formation of new reducing end-groups (Borrega, Tolonen, Bardot, Testova, & Sixta, 2013). This partial degradation of cellulose was accompanied by a slight decrease in pulp viscosity (Table 1). As for the removal of lignin, the wood chips pre-hydrolysed at higher intensities (P-factor) needed lower pulping intensities (H-factor) to reach a similar degree of delignification. The enhanced delignification of pre-hydrolysed wood is often explained by the cleavage of covalent bonds in the lignin structure during pre-hydrolysis, as well as by the increased accessibility of lignin to pulping chemicals resulting from the removal of hemicelluloses (Rauhala, King, Zuckerstätter, Suuronen, & Sixta, 2011; Yoon & van Heiningen, 2008). As shown in Table 1, increasing pre-hydrolysis intensity led to pulps with higher cellulose and lower hemicellulose contents, while the lignin content was about 3-4% in all pulps, corresponding to kappa numbers between 13 and 19. Differences in kappa number for similar lignin contents might be due to different amounts of hexenuronic acids in the pulps, as these acids are known to consume permanganate and thus affect the determination of the kappa number (Li & Gellerstedt, 1998).

**Table 1.** Yields of birch wood chips after water pre-hydrolysis, and yields and composition of unbleached pulps after kraft pulping.

Sample	P-factor	<sup>a</sup> Wood yield (%)	H-factor	<sup>a</sup> Pulp yield (%)	Cellulose (%)	Xylan (%)	<sup>b</sup> GM (%)	Lignin (%)	Kappa	Intrinsic viscosity (mL/g)
Kraft	0	100	1 000	55.5	69.2	26.7	0.4	3.8	19.4	1 346
P170	170	92.1	650	44.6	79.5	16.2	0.7	3.7	17.4	1 329
P550	550	78.3	400	37.9	87.1	9.2	0.5	3.3	13.7	1 296
P1000	1 000	74.3	200	31.0	91.3	4.8	0.3	3.5	12.8	1 237

<sup>a</sup>Wood yield after water pre-hydrolysis; pulp yield after water pre-hydrolysis and kraft pulping

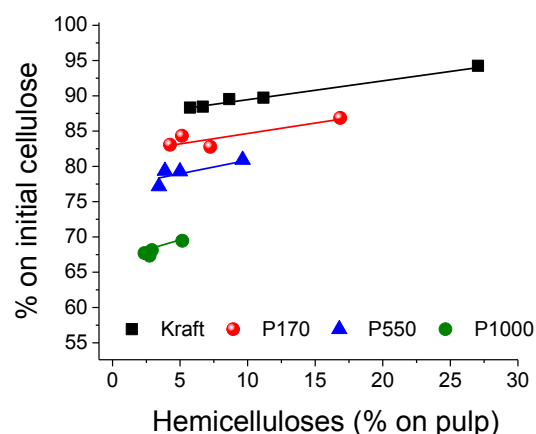
<sup>b</sup>GM: glucomannan

The unbleached kraft and PHK pulps were then subjected to water post-hydrolysis to extract the residual xylan fraction. The operational conditions for the post-hydrolysis were selected based on the results of our previous study (Borrega, Concha-Carrasco, Pranovich, & Sixta, 2017). In all pulps, the hemicelluloses (xylan) content decreased with increasing post-hydrolysis time, while the cellulose yield decreased only slightly (Fig. 1a). However, because of the partial degradation of cellulose during pre-hydrolysis and kraft pulping, the cellulose yield at a given hemicellulosic content was considerably lower in those pulps subjected to higher pre-hydrolysis intensities. For instance, at a hemicelluloses content of about 5%, the cellulose yield for the post-hydrolysed kraft pulp (without pre-hydrolysis) was about 90% of the initial cellulose in wood. In comparison, the cellulose yield for the P1000 pulp was only about 70%.

Despite the minor losses in cellulose yield with increasing post-hydrolysis time (Fig. 1a), the intrinsic viscosity of the unbleached pulps severely decreased with increasing the duration of the post-hydrolysis treatment, and thus with decreasing the hemicellulosic content (Fig. 1b). This decrease in pulp viscosity, indicating a decrease in the degree of polymerization (DP) of cellulose, was the result of hydrolytic cleavage of glycosidic bonds in the cellulose chains that occurs in high-temperature water (Bobleter, 1994). Contrary to the cellulose yield, the

intrinsic viscosity at a given xylan content was higher in those pulps subjected to higher pre-hydrolysis intensities, because these pulps had a lower initial xylan content before post-hydrolysis, and thus needed shorter post-hydrolysis times to reach a similar purity level.

a)



b)

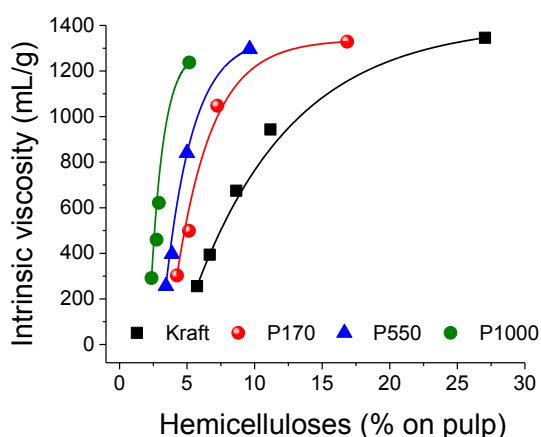


**Figure 1.** (a) Cellulose yield and (b) intrinsic viscosity of unbleached kraft and PHK pulps after water post-hydrolysis at 240 °C in a flow-through reactor, with a flow rate of 400 mL/min. The PHK pulps were pre-hydrolysed at P-factors of 170, 550 and 1000. For each pulp, different hemicellulose contents correspond to different post-hydrolysis times. Lines are included to indicate the prevailing trends.

Commercial viscose-grade pulps typically have a hemicellulosic content of about 3-6%, while their intrinsic viscosity is predominantly within the range of 400-500 mL/g. Here, based on the results from Fig. 1, selected pulps with potential for viscose conversion were bleached following a D<sub>0</sub>-E<sub>P</sub>-P sequence. The yield of the bleached pulps was not determined, but yield losses up to 5% may be expected during bleaching (Suess, 2010), particularly in those pulps with higher xylan content and/or higher amounts of low molar mass cellulose. The bleached pulps had an ISO brightness of about 83-86% (Table 2), lower than the >90% required in pulps for dissolving applications. Since it was not the purpose of this study to optimize the bleaching stages, the brightness may still be improved by selecting more appropriate bleaching sequences or by adjusting the chemical charges. This is particularly true in the case of the kraft and P1000 pulps, where an oxygen delignification stage prior to the

chlorine dioxide (D<sub>0</sub>) bleaching would be typically implemented to reduce the kappa number down to 6-8, similar to the kappa values of the post-hydrolysed pulps. On the other hand, oxygen delignification would not be recommended for pulps with low intrinsic viscosity, in order to avoid further degradation of the cellulose fraction by oxidation (Sixta, 2006). It should be mentioned that the optimization of bleaching may affect some of the chemical, molecular and structural properties of the pulps as discussed in this study. Nonetheless, the results presented in the following sections may be considered representative of the effects of pre- and post-hydrolysis on pulp properties.

The chemical composition and viscosity data of the bleached pulps is shown in Table 2. The pulp Kraft\_240.10, i.e., the kraft pulp after post-hydrolysis at 240 °C for 10 min, had a xylan content of about 7% and a viscosity of about 300 mL/g. In agreement with our previous results (Borrega & Sixta, 2013; Borrega, Concha-Carrasco, Pranovich, & Sixta, 2017), it appears that water post-hydrolysis of kraft pulp cannot lower the hemicelluloses content below 7% without compromising the pulp quality by extensive degradation of the cellulose fraction. Although the xylan content of the Kraft\_240.10 pulp was on the higher end, it may be still acceptable for viscose conversion because PHK pulps from birch containing 6-7% xylan content have previously shown satisfactory performance in a viscose process simulation (Testova et al., 2014). Moreover, although the viscosity of this pulp was relatively low, it should be sufficient for viscose conversion because in the manufacture of viscose the pulp viscosity is decreased to 230-240 mL/g by pre-aging of the alkali-cellulose. The pulps P170\_240.6 and P550\_240.3, both produced by a combination of pre- and post-hydrolysis, showed purity and viscosity values similar to those required in viscose-grade pulps (Table 2), but the need for two separate water treatments (pre- and post-hydrolysis) is not very attractive from an industrial point of view. The pulp P1000, produced only by pre-hydrolysis, showed high purity as well as high viscosity. The addition of an oxygen delignification stage prior to bleaching would probably be required to lower the viscosity to suitable levels for entering the conversion process to viscose fibers. Alternatively, the viscosity of the pulp P1000 could be adjusted with a water post-hydrolysis treatment, which not only decreases viscosity but also increases pulp purity, as shown by the properties of the P1000\_240.6 pulp in Table 2. Water post-hydrolysis of PHK pulps could be considered as an alternative method to acid hydrolysis for the adjustment of viscosity through controlled degradation of cellulose.

**Table 2.** Chemical and macromolecular properties of bleached kraft pulp and selected pre- and post-hydrolyzed pulps. Pre-hydrolysis was conducted at 170 °C at different intensities (P-factor), while post-hydrolysis was conducted at 240 °C and various treatment times.

	Kraft	Kraft 240.10	P170 240.6	P550 240.3	P1000	P1000 240.6
P-factor	0	0	170	550	1 000	1 000
Post-hydrolysis time (min)	0	10	6	3	0	6
Cellulose (% on pulp)	73.6	93.2	94.9	94.6	95.4	97.2
Xylan (% on pulp)	26.4	6.8	5.1	5.4	4.6	2.8
ISO brightness (%)	82.7	84.2	83.3	83.7	86.4	84.0
Intrinsic viscosity (mL/g)	969	296	356	507	671	324
Mw (kg/mol)	770	163	218	308	464	178
PDI	11.6	2.8	3.0	3.6	5.8	2.8
DP > 2000	0.48	0.12	0.19	0.29	0.37	0.14
DP < 100	0.05	0.05	0.03	0.03	0.04	0.01

In addition to viscosity values, the macromolecular properties of the selected bleached pulps were further studied by determining their molar mass distribution by GPC (Fig. 2). The peak in the low molar mass region, corresponding to the hemicelluloses, was clearly visible for the kraft pulp but largely disappeared from the molar

mass distribution of all water-treated pulps. The peak corresponding to the cellulose fraction shifted towards lower molar mass regions by increasing the intensity of the pre-hydrolysis and/or post-hydrolysis treatment. The degradation of cellulose was also evident by a decrease in the weight average molar mass ( $M_w$ ) and in the number of molecules with a  $DP > 2000$  (Table 2). The pulp P1000\_240.6 had the lowest amount of molecules with  $DP < 100$ , while the pulps produced by pure pre-hydrolysis (P1000) or pure post-hydrolysis (Kraft\_240.10), together with the kraft pulp, had the highest amount of this  $DP < 100$  fraction. The presence of these short-chain molecules in the pulp, originating from the hemicelluloses and from degraded cellulose fragments, appears to have a negative effect on the mechanical properties of viscose fibers (Sixta, 2006). Finally, increasing the intensity of the hydrothermal treatment resulted in pulps with narrower molar mass distribution (see Fig. 2 and PDI values in Table 2), a desired feature in dissolving pulps because it relates to the homogeneity of the cellulosic material.

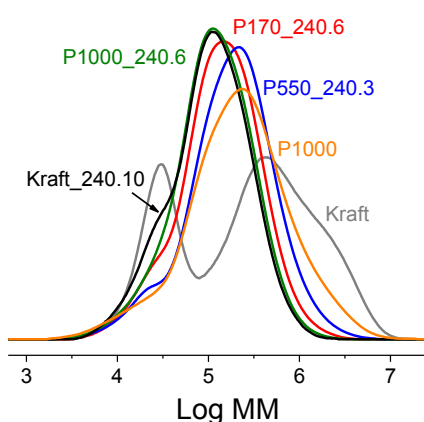


**Figure 2.** Molar mass distribution of bleached kraft pulp and selected pre- and post-hydrolysed pulps. Pre-hydrolysis was performed at P-factors of 0, 170, 550 and 1000, while post-hydrolysis was performed at 240 °C for 3, 6 or 10 min.

### 3.2. Supramolecular pulp properties

The supramolecular structure of the bleached pulps was investigated by solid state NMR and WAXS. The NMR data showed that the lateral fibril dimension (LFD), a measure of the cellulose crystallite size, was about 4-5 nm in all pulps (Table 3). These values were in agreement with published data on fibril dimensions in kraft pulps produced under different pulping conditions (Duchesne et al., 2001; Virtanen, Liisa Maunu, Tamminen, Hortling, & Liitiä, 2008). The LFD appeared to increase slightly from 3.9 nm in the kraft pulp to 4.1 nm in the P1000 pulp. Interestingly, all pulps that were subjected to post-hydrolysis clearly showed a higher LFD, with values around 4.5-4.7 nm. It has been previously reported that water pre-hydrolysis of birch wood induces an increase in the cellulose crystal size, particularly with increasing pre-hydrolysis temperature (Penttilä et al., 2013; Testova et al., 2014). The increase in crystal size in both pre- and post-hydrolyzed pulps might be explained by the crystallization of cellulose chains on the surfaces of the crystals as well as by agglomeration (coalescence) of neighboring cellulose chains. These molecular re-arrangements would be favored in the presence of water (plasticizer), and further promoted by the use of elevated temperatures during the hydrothermal treatment (Atalla, Ellis, & Schroeder, 1984). Nonetheless, the crystallization or coalescence of cellulose chains would probably imply the splitting and thus shrinking of neighboring crystallites, which would then leave the average LFD unchanged. At this stage, the mechanism for the increase in LFD still remains unclear. In any case, the increase in LFD was also

accompanied by an increase in cellulose crystallinity, from 50% for the kraft pulp to about 57% for all post-hydrolyzed pulps (Table 3). These crystallinity values are well in agreement with several studies on the supramolecular structure of kraft and PHK pulps (Hult, Liitiä, Maunu, Hortling, & Iversen, 2002; Wollboldt, Zuckerstätter, Weber, Larsson, & Sixta, 2010; Testova et al., 2014). The differences in the supramolecular structure of cellulose in the kraft, pre-hydrolyzed, and post-hydrolyzed pulps were evident from the recorded NMR spectra originating from the C4 carbon (supporting information).

**Table 3.** Supramolecular properties of bleached kraft pulp and selected pre- and post-hydrolyzed pulps. Pre-hydrolysis was conducted at 170 °C at different intensities (P-factor), while post-hydrolysis was conducted at 240 °C and various treatment times.

	Kraft	Kraft_240.10	P170_240.6	P550_240.3	P1000	P1000_240.6
<i>Solid state NMR</i>						
Crystallinity index ( $\pm 1\%$ )	50 $\pm$ 1	57 $\pm$ 1	57 $\pm$ 1	57 $\pm$ 1	52 $\pm$ 1	56 $\pm$ 1
Lateral fibril dimension ( $\pm 0.1$ nm)	3.9	4.6	4.7	4.6	4.1	4.5
Aggregate dimension (nm)	37 $\pm$ 4	27 $\pm$ 2	28 $\pm$ 2	26 $\pm$ 1	22 $\pm$ 1	24 $\pm$ 1
Specific surface area (m <sup>2</sup> /g)	73 $\pm$ 9	99 $\pm$ 6	95 $\pm$ 6	104 $\pm$ 5	119 $\pm$ 4	113 $\pm$ 6
<i>X-ray diffraction</i>						
Crystallinity (%)						
Sample	45	53	51	50	46	52
Cellulose	61.1	56.9	53.7	52.9	48.2	53.5
Crystal width ( $\pm 0.5$ nm)						
1-10	4.1	4.0	4.2	4.0	3.8	4.1
110	3.9	4.7	4.8	4.9	5.2	5.0
200	4.0	5.0	5.0	4.9	4.3	5.0

Cellulose fibrils in the fiber cell wall tend to aggregate and form larger structures, typically called microfibrils. Here, the fibrils in the kraft pulp formed the largest aggregates, as indicated by the lateral fibril aggregate dimensions (LFAD), while the P1000 pulp had the smallest aggregates despite having rather similar fibril dimensions as the kraft pulp (Table 3). It has been reported that pulps produced by an alkaline process tend to show larger aggregates than those produced or subjected to an acidic treatment (Wollboldt et al., 2010). The acidic conditions generated during water pre-hydrolysis of wood may thus explain the difference in aggregate dimensions between the kraft and P1000 pulp samples. It should also be mentioned that the aggregate dimensions for the kraft pulp (37 nm) were significantly higher than the 15-25 nm commonly found in pulps (Hult, Larsson, & Iversen, 2001; Hult, Liitiä, Maunu, Hortling, & Iversen, 2002; Wollboldt, Zuckerstätter, Weber, Larsson, & Sixta, 2010). The kraft pulp in this study was bleached with a rather unconventional bleaching sequence, with the absence of an oxygen delignification stage, and this might have had an effect on fibril aggregation. According to the fibrillar model used for the determination of the supramolecular structure in cellulose I, the surface of the fibrils are assumed to be easily accessible while the inner surfaces may have restricted access due to aggregation. The specific surface area (SSA) in the wet state, which was computed from the LFAD, obviously showed that the SSA was the lowest for the kraft pulp and the highest for the P1000 pulp, with SSA values for all post-hydrolyzed pulps laying in between.

In general, qualitative variations in the supramolecular structure of cellulose detected by NMR tend to agree well to those detected by x-ray scattering, even if the absolute values determined by these methods may differ (Lee et al., 2016). The results from the WAXS analyses showed that the cellulose crystal size measured from the 200 reflection increased slightly from 4 nm in the kraft pulp to 4.3 nm in the P1000 pulp, with all post-hydrolyzed

samples showing a significantly higher crystal size, about 5 nm (Table 3). In the 110 direction, the crystal size was larger in all water-treated pulps than in the kraft pulp, while in the 1-10 direction the size was similar in all pulps. The differences in the crystalline structure of cellulose, particularly in the 200 reflection, between the post-hydrolysed pulps and the kraft and P1000 pulps could be seen from the WAXS spectra (supplementary material). Overall, the crystallite dimensions and their increase with increasing the intensity of the hydrothermal treatment were in close agreement with those determined by NMR.

The sample crystallinity determined by WAXS was between 45-53%, increasing slightly from the kraft to the P1000 pulp, and then further in the post-hydrolyzed pulps. By taking into account the chemical composition of the pulps, the degree of cellulose crystallinity could also be estimated. In all pre- and post-hydrolyzed pulps, with a high cellulose content (>93%), the cellulose crystallinity was similar to the sample crystallinity. Moreover, the cellulose crystallinity determined by WAXS was in good agreement with the crystallinity values from the NMR measurements (Table 3). In the kraft pulp, however, the cellulose crystallinity estimated by WAXS (61%) was considerably higher than that determined by NMR (50%). It is well known that the presence of amorphous polymers such as hemicelluloses interfere with the spectral fitting for the determination of crystallinity in NMR experiments, and thus the removal of hemicelluloses by acid hydrolysis is often performed prior to the analyses (Hult, Larsson, & Iversen, 2000; Liitiä et al., 2003). In order to avoid any hydrolytic degradation of the cellulose fraction, the removal of hemicelluloses from the kraft pulp was not performed in this study, which might have affected the determination of crystallinity.

### *3.3. Accessibility and reactivity of pulps*

Probably the most important property of any dissolving-grade pulp is its reactivity, that is, how well the pulp reacts (dissolves) in a particular chemical solvent system so it can be transformed into the desired final product. The pulp reactivity depends on a variety of chemical, molecular and fibrillar features, but it is strongly related to the accessibility of functional groups in the pulp, mainly -OH groups (Sixta, 2006). In this study, the accessibility of -OH groups was determined after deuteration of the samples at 95% RH in a D<sub>2</sub>O atmosphere. This relative humidity should be enough to reach complete exchange of free -OH groups into -OD groups, as it has been previously shown that the deuterium exchange in wood reaches a maximum at 60% RH (Taniguchi, Harada, & Nakato, 1978).

The accessibility values for our pulp samples are shown in Table 4. All post-hydrolyzed pulps had a similar accessibility, with 54-58% of their -OH groups being reactive. The P1000 pulp clearly had the highest accessibility, which was probably related to its high SSA, derived from the presence of small fibril aggregates. On the other hand, the accessibility of the kraft pulp was lower than that of the P1000 pulp, but higher than that of the post-hydrolyzed pulps (Table 4). The fibril aggregates in the kraft pulp appeared to be the largest, and correspondingly its SSA was the lowest. Therefore, the high accessibility of the kraft pulp may be related to its high xylan content, because hemicelluloses are amorphous polymers with free -OH groups. It should also be mentioned that in the case of the P1000 and kraft pulps, their accessibility values might be slightly underestimated, because at the end of the deuteration stage (10 hours) the pulp mass did not seem to have reached yet an equilibrium (dm/dt was about 0.001-0.0015%, compared to <0.0008% for the post-hydrolyzed pulps). Nonetheless, differences in accessibility values with extending deuteration time might be expected to be rather small.

**Table 4.** Accessible hydroxyl (-OH) groups and reactivity values of bleached kraft pulp and selected pre- and post-hydrolysed pulps. Pre-hydrolysis was conducted at 170 °C at different intensities (P-factor), while post-hydrolysis was conducted at 240 °C and various treatment times. The reference pulp is a commercial bleached birch pulp produced by PHK pulping.

	-OH groups (mmol/g pulp)	-OH groups (% on total)	Fock reactivity (%)	DTR reactivity	
				IDR ( $\mu\text{Nm/s}$ )	T0.1 (s)
Kraft	$11.2 \pm 0.4$	63.5	$30 \pm 1.7$	$1.92 \pm 0.09$	$1\ 518 \pm 19$
Kraft_240.10	$10.7 \pm 0.4$	58.3	$21 \pm 3.8$	$0.17 \pm 0.04$	$258 \pm 3$
P170_240.6	$10.6 \pm 0.4$	57.9	$14 \pm 3.9$	$0.21 \pm 0.01$	$305 \pm 5$
P550_240.3	$10.0 \pm 0.1$	54.3	nd	nd	nd
P1000	$12.1 \pm 0.2$	65.9	$15 \pm 2.3$	$0.40 \pm 0.04$	$657 \pm 8$
P1000_240.6	$10.6 \pm 0.3$	57.5	$18 \pm 2.9$	$0.23 \pm 0.06$	$267 \pm 8$
Reference	$10.2 \pm 0.0$	55.8	$20 \pm 1.4$	$0.24 \pm 0.01$	$415 \pm 9$

The proportion of accessible -OH groups in the reference (commercial) pulp was lower than that in the P1000 pulp, despite the fact that both pulps were produced by PHK pulping of birch wood. However, the process parameters during pre-hydrolysis, pulping and bleaching differed, which may have affected the accessibility of the pulp. Moreover, the reference pulp was delivered in dry sheets, and was re-wetted in liquid water before the DVS experiments. This additional re-wetting and drying cycle probably reduced the accessibility of -OH groups, due to irreversible hydrogen bonding caused by the closure of pores during water removal (i.e. hornification) (Weise, 1998).

In this study, the reactivity of the pulps in a viscose conversion process was first estimated by the Fock method, which quantified the amount of regenerated cellulose in the xanthate. All post-hydrolyzed samples gave similar amounts of regenerated cellulose, as indicated by the Fock reactivity values in Table 4. Moreover, the pulp P1000 also showed similar reactivity than the post-hydrolyzed pulps, even though its accessibility was considerably higher. The Fock reactivity appears to decrease with increasing the molar mass of the cellulose fraction (Engström et al., 2006), and thus the higher molar mass of the P1000 pulp, compared to the post-hydrolyzed pulps, may have resulted in lower Fock values than otherwise expected from the accessibility of its -OH groups. For all dissolving-grade pulps, including the commercial (reference) PHK pulp, the reactivity was less than 25% (Table 4), much lower than previously reported for other hardwood PHK pulps (Duan et al., 2015; Miao et al., 2014). In the absence of detailed information on experimental parameters during the Fock tests, we can only assume that the reactivity of our pulp samples was strongly affected by the testing conditions (Tian et al., 2013). Surprisingly, the kraft pulp was the most reactive sample, even though both its molar mass and xylan content were the highest. It is well established that kraft pulps exhibit poor reactivity during viscose conversion, mainly because the hemicelluloses react with the derivatizing chemicals and impair the conversion of cellulose (Gehmayr et al., 2011; Wollboldt et al., 2010). Therefore, the results from the Fock tests should be interpreted with caution, as they may not be representative of the true behavior of the pulps in a viscose process.

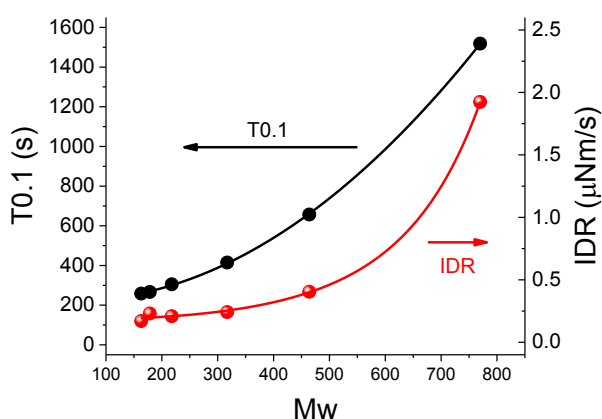


**Figure 3.** Initial dissolution rate (IDR) and time to complete dissolution (T0.1) of bleached kraft, pre- and post-hydrolyzed pulp samples in CED solvent, plotted as a function of their average weight molar mass (Mw).

The pulp reactivity to derivatizing chemicals was alternatively investigated by monitoring its rheological behavior during dissolution in CED. According to this method, a pulp shows high reactivity if the initial dissolution rate (IDR) is high and the time to complete dissolution (T0.1) is short (Ceccherini & Maloney, 2017). Interestingly, the results in Table 4 indicate that those pulps with a high IDR also showed a high T0.1. In other words, the pulps that started dissolving at a fast pace required longer time to complete the dissolution process. The pulps could be roughly classified into three categories, with kraft pulp showing the highest IDR and T0.1 values, followed by the P1000 pulp and then by all post-hydrolyzed pulps. As shown in Fig. 3, the reactivity parameters determined by the DTR test were strongly related to the molar mass of the pulp. Adjusting the pulp viscosity prior to the reactivity tests may thus be required in order to evaluate the effect of other physical and chemical pulp properties on their reactivity. It should also be considered that the accessibility and reactivity parameters of the pulps determined in this study may differ if some pulp properties were adjusted by selecting different bleaching conditions.

### 3.4. Recovery of xylan-based sugars from the aqueous hydrolysates

The side-streams generated during the hydrothermal treatments of wood and pulp were analyzed to determine their chemical composition (Table 5). In pre-hydrolysis, increasing the P-factor led to higher amounts of xylan-derived sugars, although the share of oligo- and/or polysaccharides ( $DP \geq 2$ ) decreased due to their degradation under elevated temperature and prolonged reaction times (Borrega, Niemela, & Sixta, 2013; Liu, Li, Luo, Chen, & Huang, 2015). Other sugars originating from the partial degradation of glucomannan and cellulose, as well as a soluble lignin fraction were also present in the hydrolysates. It is likely that several degradation products such as furans and carboxylic acids were also formed, particularly with increasing pre-hydrolysis intensity (Borrega, Niemela, & Sixta, 2013), but were not here analyzed. At a P-factor of 1000, almost 11% of xylose (based on dry wood) was found in the pre-hydrolysate, with half of it in oligo- and/or polymeric form. These values were well in agreement with previous reports on xylose yields during water autohydrolysis of birch wood (Testova et al., 2011).

In the post-hydrolysates, the amount of xylan-based sugars decreased with increasing pre-hydrolysis intensity. This was obviously a direct consequence of lower xylan content in the unbleached pulps and shorter post-hydrolysis times needed for pulps pre-hydrolyzed at higher P-factor. Since water post-hydrolysis was performed



in a flow-through reactor and under high flow rates, the xylan-based compounds were found quantitatively as oligo- and/or polymers (Table 5). In pure post-hydrolysis (Kraft\_240.10), the amount of xylose recovered from the hydrolysate was about 10% on initial dry wood, similar to the amount of xylose (11%) recovered from pure pre-hydrolysis (P1000), and for a similar amount of residual xylan (5-7%) in the pulp. The xylose in the post-hydrolysate for the Kraft\_240.10 sample corresponded to about 17% of the dry pulp mass, slightly lower than the 20% previously reported under similar conditions of temperature, time and flow (Borrega, Concha-Carrasco, Pranovich, & Sixta, 2017). In those treatments with combined pre- and post-hydrolysis, the total recovery of xylose was dependent on the pre-hydrolysis intensity. At a P-factor of 550, about 10-11% of xylan-based sugars (on dry wood) were also found in the aqueous hydrolysates, but at a P-factor of 170, only about 7% of xylan-based sugars were found. This lower recovery may be explained by extensive xylan dissolution during alkaline pulping, following the cleavage of xylan chains in wood during the low-intensity pre-hydrolysis.

**Table 5.** Chemical and macromolecular composition of selected aqueous pre- and post-hydrolysates. Pre-hydrolysis was conducted at 170 °C at different intensities (P-factor), while post-hydrolysis was conducted at 240 °C and various treatment times. The amounts of sugars and lignin are shown as % on initial birch wood, unless otherwise indicated.

	Kraft_240.10	P170_240.6	P550_240.3	P1000	P1000_240.6
<i>Pre-hydrolysate</i>					
Total xylose (%)	na	3.1	9.2	10.9	10.9
DP $\geq 2$ (% of xylose)	na	96.1	88.2	49.5	49.5
Mw (kDa)	na	nd	nd	1.2	1.2
PDI	na	nd	nd	1.4	1.4
Concentration (g/L)	na	7.8	22.9	27.2	27.2
Other sugars (%)	na	1.2	2.0	2.3	2.3
Soluble lignin (%)	na	1.8	2.9	2.6	2.6
<i>Post-hydrolysate</i>					
Total xylose (%)	9.8	4.0	1.3	na	0.6
DP $\geq 2$ (% of xylose)	>99	>99	>99	na	>99
Mw (kDa)	10.5	nd	nd	na	nd
PDI	3.4	nd	nd	na	nd
Concentration (g/L)	0.6	0.5	0.2	na	0.1
Other sugars (%)	0.3	0.1	<0.1	na	0.1
Soluble lignin (%)	0.4	0.6	nd	na	0.2

Despite similar xylose recovery by pure pre- and post-hydrolysis, the molar mass of the xylan-based compounds in the pre- and post-hydrolysates clearly differed. Since these compounds were the most abundant in the hydrolysates, it was assumed that the molar masses of the dissolved products largely corresponded to those of the xylan-based sugars. In pre-hydrolysis (P1000), their average molar mass (Mw) was about 1.2 kDa, while in post-hydrolysis the xylan had an average molar mass of about 10.5 kDa (Table 5). The molar mass distribution was also broader for the xylan-based compounds in the post-hydrolysate, as indicated by the polydispersity index (PDI). According to the molar mass characteristics, the xylan fraction in the post-hydrolysates may be utilized as multifunctional food ingredient to improve several technological properties in dairy products and to promote health-related effects (Rosa-Sibakov et al., 2016). Moreover, the amount of impurities (other sugars, lignin) was less than 1% on wood in the Kraft\_240.10 post-hydrolysate, compared to the 5% found in the P1000 pre-hydrolysate. The higher purity of the xylan fraction in the post-hydrolysates was probably related to the more homogeneous composition of pulp, as compared to wood, and thus it may be expected to facilitate its recovery using membrane filtration techniques. It should be mentioned, however, that the concentration of xylan-based

sugars in the post-hydrolysates was very low (less than 1g/L), and thus their isolation by membrane filtration would be a highly energy intensive process. Lowering the flow rate in post-hydrolysis may increase the product concentration, but then the total amount of sugars recovered would be lower (Borrega et al., 2017). More data on xylan yields at different flow rates, energy requirements for isolation, and product market price would be needed to assess the economic viability of the recovery process.

#### **4. Conclusions**

Water post-hydrolysis of kraft pulp can produce viscose-grade pulp with considerably higher cellulose yield than traditional PHK pulping, but the pulp viscosity at a given hemicellulosic content is considerably lower. This fact limits the application of water post-hydrolysis, particularly on high-hemicellulose containing pulps, because high purity levels cannot be reached without compromising the cellulose quality. Compared to pre-hydrolysis, water post-hydrolysis results in lower accessibility of hydroxyl groups, probably derived from supramolecular re-arrangements in cellulose promoted by high-temperature water. Despite the lower accessibility, the reactivity of post-hydrolysed pulps to derivatising chemicals is not seemingly compromised. However, the bleached pulps in this study did not reach all the required specifications (e.g. brightness) for the viscose process, and thus the variation in some pulp properties by adjusting the bleaching operation may in turn alter the accessibility and reactivity of the pulps. Moreover, the performance of the pulps during the actual conversion to viscose needs yet to be assessed to clearly elucidate the suitability of post-hydrolysed pulps for the viscose process. The use of a flow-through system for pulp post-hydrolysis allows the recovery of a high purity and molar mass xylan fraction for high-value applications.

#### **Supplementary materials**

E-supplementary data of this work can be found in the online version of the paper.

#### **Acknowledgements**

This work was supported by the Academy of Finland through the PURCELL project (decision number 275398). Mr. Atte Mikkelsen (VTT Technical Research of Finland Ltd.) is thanked for performing the SEC analyses of aqueous hydrolysates, and Dr. Tiina Liitiä (VTT) is thanked for valuable discussions on the manuscript.

## References

- Ahvenainen, P., Kontro, I., & Svedström, K. (2016). Comparison of sample crystallinity determination methods by X-ray diffraction for challenging cellulose I materials. *Cellulose*, 23(2), 1073–1086. <https://doi.org/10.1007/s10570-016-0881-6>
- Alonso, D. M., Hakim, S. H., Zhou, S., Won, W., Hosseinaei, O., Tao, J., ... Dumesic, J. A. (2017). Increasing the revenue from lignocellulosic biomass: Maximizing feedstock utilization. *Science Advances*, 3(5), E1603301. <https://doi.org/10.1126/sciadv.1603301>
- Atalla, R. H., Ellis, J. D., & Schroeder, L. R. (1984). Some effects of elevated temperatures on the structure of cellulose and its transformation. *Journal of Wood Chemistry and Technology*, 4(4), 465–482. <https://doi.org/10.1080/02773818408070662>
- Bobleter, O. (1994). Hydrothermal degradation of polymers derived from plants. *Progress in Polymer Science*, 19(5), 797–841. [https://doi.org/10.1016/0079-6700\(94\)90033-7](https://doi.org/10.1016/0079-6700(94)90033-7)
- Borrega, M., Concha-Carrasco, S., Pranovich, A., & Sixta, H. (2017). Hot water treatment of hardwood kraft pulp produces high-purity cellulose and polymeric xylan. *Cellulose*. <https://doi.org/10.1007/s10570-017-1462-z>
- Borrega, M., Niemela, K., & Sixta, H. (2013). Effect of hydrothermal treatment intensity on the formation of degradation products from birchwood. *Holzforschung*, 67(8), 871–879. <https://doi.org/10.1515/hf-2013-0019>
- Borrega, M., & Sixta, H. (2013). Purification of cellulosic pulp by hot water extraction. *Cellulose*, 20(6), 2803–2812. <https://doi.org/10.1007/s10570-013-0086-1>
- Borrega, M., Tolonen, L. K., Bardot, F., Testova, L., & Sixta, H. (2013). Potential of hot water extraction of birch wood to produce high-purity dissolving pulp after alkaline pulping. *Bioresource Technology*, 135, 665–671. <https://doi.org/10.1016/j.biortech.2012.11.107>
- Bozell, J. J., Black, S. K., Myers, M., Cahill, D., Miller, W. P., & Park, S. (2011). Solvent fractionation of renewable woody feedstocks: Organosolv generation of biorefinery process streams for the production of biobased chemicals. *Biomass and Bioenergy*, 35(10), 4197–4208. <https://doi.org/10.1016/j.biombioe.2011.07.006>
- Ceccherini, S., & Maloney, T. (2017). Novel CED-based rheological test to evaluate pulp reactivity. In 16th Fundamental Research Symposium (pp. 909–927). Oxford.
- Christoffersson, K. E., Sjöström, M., Edlund, U., Lindgren, A., & Dolk, M. (2002). Reactivity of dissolving pulp: characterisation using chemical properties, NMR spectroscopy and multivariate data analysis. *Cellulose*, 9(2), 159–170. <https://doi.org/10.1023/A:1020108125490>
- Deutschmann, R., & Dekker, R. F. H. (2012). From plant biomass to bio-based chemicals: Latest developments in xylan research. *Biotechnology Advances*, 30(6), 1627–1640. <https://doi.org/10.1016/j.biotechadv.2012.07.001>

560 Duan, C., Li, J., Ma, X., Chen, C., Liu, Y., Stavik, J., & Ni, Y. (2015). Comparison of acid sulfite (AS)- and  
 561 prehydrolysis kraft (PHK)-based dissolving pulps. *Cellulose*, 22(6), 4017–4026.  
 562 <https://doi.org/10.1007/s10570-015-0781-1>

563 Duchesne, I., Hult, E., Molin, U., Daniel, G., Iversen, T., & Lennholm, H. (2001). The influence of hemicellulose  
 564 on fibril aggregation of kraft pulp fibres as revealed by FE-SEM and CP/MAS 13C-NMR. *Cellulose*, 8(2),  
 565 103–111. <https://doi.org/10.1023/A:1016645809958>

566 Engström, A. C., Ek, M., & Henriksson, G. (2006). Improved accessibility and reactivity of dissolving pulp for  
 567 the viscose process: Pretreatment with monocomponent edoglucanase. *Biomacromolecules*, 7(6), 2027–  
 568 2031. <https://doi.org/10.1021/bm0509725>

569 FAO Yearbook of Forest Products, 2007. <http://www.fao.org/3/a-i0750m.pdf>

570 FAO Yearbook of Forest Products, 2015. <http://www.fao.org/3/a-i7304m.pdf>

571 Froschauer, C., Hummel, M., Iakovlev, M., Roselli, A., Schottenberger, H., & Sixta, H. (2013). Separation of  
 572 hemicellulose and cellulose from wood pulp by means of ionic liquid/cosolvent systems.  
 573 *Biomacromolecules*, 14(6), 1741–1750. <https://doi.org/10.1021/bm400106h>

574 Gehmayr, V., Schild, G., & Sixta, H. (2011). A precise study on the feasibility of enzyme treatments of a kraft  
 575 pulp for viscose application. *Cellulose*, 18(2), 479–491. <https://doi.org/10.1007/s10570-010-9483-x>

576 Hansen, N. M. L., & Plackett, D. (2008). Sustainable films and coatings from hemicelluloses: A review.  
 577 *Biomacromolecules*, 9(6), 1493–1505. <https://doi.org/10.1021/bm800053z>

578 Hult, E. L., Larsson, P. T., & Iversen, T. (2000). Comparative CP/MAS 13C-NMR study of cellulose structure in  
 579 spruce wood and kraft pulp. *Cellulose*, 7(1), 35–55. <https://doi.org/10.1023/A:1009236932134>

580 Hult, E. L., Larsson, P. T., & Iversen, T. (2001). Cellulose fibril aggregation - An inherent property of kraft pulps.  
 581 *Polymer*, 42(8), 3309–3314. [https://doi.org/10.1016/S0032-3861\(00\)00774-6](https://doi.org/10.1016/S0032-3861(00)00774-6)

582 Hult, E. L., Liitiä, T., Maunu, S. L., Hortling, B., & Iversen, T. (2002). A CP/MAS 13C-NMR study of cellulose  
 583 structure on the surface of refined kraft pulp fibers. *Carbohydrate Polymers*, 49(2), 231–234.  
 584 [https://doi.org/10.1016/S0144-8617\(01\)00309-5](https://doi.org/10.1016/S0144-8617(01)00309-5)

585 Iakovlev, M., You, X., van Heiningen, A., & Sixta, H. (2014). SO<sub>2</sub>-ethanol-water (SEW) fractionation process:  
 586 Production of dissolving pulp from spruce. *Cellulose*, 21(3), 1419–1429. <https://doi.org/10.1007/s10570-014-0202-x>

587

588 Ibarra, D., Köpcke, V., & Ek, M. (2009). Exploring enzymatic treatments for the production of dissolving grade  
 589 pulp from different wood and non-wood paper grade pulps. *Holzforschung*, 63(6), 721–730.  
 590 <https://doi.org/10.1515/HF.2009.102>

591 Janson, J. (1970). Calculation of the polysaccharide composition of wood and pulp. *Paperi Ja Puu - Paper and*  
 592 *Timber*, 52(5), 323–329.

593 Janzon, R., Puls, J., & Saake, B. (2006). Upgrading of paper-grade pulps to dissolving pulps by nitren extraction:  
 594 Optimisation of extraction parameters and application to different pulps. *Holzforschung*, 60(4), 347–354.  
 595 <https://doi.org/10.1515/HF.2006.055>

596 Koivula, E., Kallioinen, M., Preis, S., Testova, L., Sixta, H., & Mänttari, M. (2011). Evaluation of various  
 597 pretreatment methods to manage fouling in ultrafiltration of wood hydrolysates. *Separation and Purification*  
 598 *Technology*, 83(1), 50–56. <https://doi.org/10.1016/j.seppur.2011.09.006>

599 Larsson, P. T., Wickholm, K., & Iversen, T. (1997). A CP/MAS carbon-13 NMR investigation of molecular  
 600 ordering in celluloses. *Carbohydrate Research*, 302(1–2), 19–25. [https://doi.org/10.1016/S0008-](https://doi.org/10.1016/S0008-6215(97)00130-4)  
 601 [6215\(97\)00130-4](https://doi.org/10.1016/S0008-6215(97)00130-4)

602 Lê, H. Q., Ma, Y., Borrega, M., & Sixta, H. (2016). Wood biorefinery based on  $\gamma$ -valerolactone/water  
 603 fractionation. *Green Chemistry*, 18(20), 5466–5476. <https://doi.org/10.1039/C6GC01692H>

604 Lee, C., Dazen, K., Kafle, K., Moore, A., Johnson, D.K., Park, S., Kim, S.H., 2016. Correlations of apparent  
 605 cellulose crystallinity determined by XRD, NMR, IR, Raman, and SFG methods. *Advances in Polymer*  
 606 *Science*, 271, 115-132. [https://doi.org/10.1007/12\\_2015\\_320](https://doi.org/10.1007/12_2015_320)

607 Li, J., & Gellerstedt, G. (1998). On the structural significance of the kappa number measurement. *Nordic Pulp*  
 608 *and Paper Research Journal*, 13(2), 153–158. <https://doi.org/10.3183/NPPRJ-1998-13-02-p153-158>

609 Liitiä, T., Maunu, S. L., Hortling, B., Tamminen, T., Pekkala, O., & Varhimo, A. (2003). Cellulose crystallinity  
 610 and ordering of hemicelluloses in pine and birch pulps as revealed by solid-state NMR spectroscopic  
 611 methods. *Cellulose*, 10(4), 307–316. <https://doi.org/10.1023/A:1027302526861>

612 Liu, J., Li, M., Luo, X., Chen, L., & Huang, L. (2015). Effect of hot-water extraction (HWE) severity on bleached  
 613 pulp based biorefinery performance of eucalyptus during the HWE-Kraft-ECF bleaching process.  
 614 *Bioresource Technology*, 181, 183–190. <https://doi.org/10.1016/j.biortech.2015.01.055>

615 Liu, Y., Shi, L., Cheng, D., & He, Z. (2016). Dissolving pulp market and technologies: Chinese prospective - a  
 616 mini-review. *BioResources*, 11(3), 7902–7916. <https://doi.org/10.15376/biores.11.3.Liu>

617 Miao, Q., Chen, L., Huang, L., Tian, C., Zheng, L., & Ni, Y. (2014). A process for enhancing the accessibility  
 618 and reactivity of hardwood kraft-based dissolving pulp for viscose rayon production by cellulase treatment.  
 619 *Bioresource Technology*, 154, 109–113. <https://doi.org/10.1016/j.biortech.2013.12.040>

620 Nishiyama, Y., Langan, P., & Chanzy, H. (2002). Crystal structure and hydrogen-bonding system in cellulose I $\beta$   
 621 from synchrotron X-ray and neutron fiber diffraction. *Journal of the American Chemical Society*, 124(31),  
 622 9074–9082. <https://doi.org/10.1021/ja0257319>

623 Penttilä, P. A., Kilpeläinen, P., Tolonen, L., Suuronen, J. P., Sixta, H., Willför, S., & Serimaa, R. (2013). Effects  
 624 of pressurized hot water extraction on the nanoscale structure of birch sawdust. *Cellulose*, 20(5), 2335–  
 625 2347. <https://doi.org/10.1007/s10570-013-0001-9>

626   Rauhala, T., King, A. W. T., Zuckerstätter, G., Suuronen, S., & Sixta, H. (2011). Effect of autohydrolysis on the  
627       lignin structure and the kinetics of delignification of birch wood. *Nordic Pulp and Paper Research Journal*,  
628       26(4), 386–391. <https://doi.org/10.3183/NPPRJ-2011-26-04-p386-391>

629   Rosa-Sibakov, N., Hakala, T. K., Sözer, N., Nordlund, E., Poutanen, K., & Aura, A. M. (2016). Birch pulp xylan  
630       works as a food hydrocolloid in acid milk gels and is fermented slowly in vitro. *Carbohydrate Polymers*,  
631       154, 305–312. <https://doi.org/10.1016/j.carbpol.2016.06.028>

632   Roselli, A., Hummel, M., Monshizadeh, A., Maloney, T., & Sixta, H. (2014). Ionic liquid extraction method for  
633       upgrading eucalyptus kraft pulp to high purity dissolving pulp. *Cellulose*, 21(5), 3655–3666.  
634       <https://doi.org/10.1007/s10570-014-0344-x>

635   Sixta, H. (2006). *Handbook of Pulp*. Wiley-VCH.

636   Suess, H. U. (2010). Bleaching of chemical pulp. In H. U. Suess (ed.), *Pulp Bleaching Today* (pp. 45-199). Walter  
637       de Gruyter.

638   Song, T., Pranovich, A., Sumerskiy, I., & Holmbom, B. (2008). Extraction of galactoglucomannan from spruce  
639       wood with pressurised hot water. *Holzforschung*, 62(6), 659–666. <https://doi.org/10.1515/HF.2008.131>

640   Taniguchi, T., Harada, H., & Nakato, K. (1978). Determination of water adsorption sites in wood by a hydrogen–  
641       deuterium exchange. *Nature*, 272(5650), 230–231. <https://doi.org/10.1038/272230a0>

642   Testova, L., Borrega, M., Tolonen, L. K., Penttilä, P. A., Serimaa, R., Larsson, P. T., & Sixta, H. (2014).  
643       Dissolving-grade birch pulps produced under various prehydrolysis intensities: Quality, structure and  
644       applications. *Cellulose*, 21(3), 2007–2021. <https://doi.org/10.1007/s10570-014-0182-x>

645   Testova, L., Chong, S. L., Tenkanen, M., & Sixta, H. (2011). Autohydrolysis of birch wood. *Holzforschung*, 65(4),  
646       535–542. <https://doi.org/10.1515/HF.2011.073>

647   Tian, C. ., Zheng, L. ., Miao, Q. ., Nash, C. ., Cao, C. ., & Ni, Y. . (2013). Improvement in the Fock test for  
648       determining the reactivity of dissolving pulp. *Tappi Journal*, 12(11), 21–26.

649   Virtanen, T., Liisa Maunu, S., Tamminen, T., Hortling, B., & Liitiä, T. (2008). Changes in fiber ultrastructure  
650       during various kraft pulping conditions evaluated by <sup>13</sup>C CPMAS NMR spectroscopy. *Carbohydrate*  
651       *Polymers*, 73(1), 156–163. <https://doi.org/10.1016/j.carbpol.2007.11.015>

652   Vroom, K. E. (1957). The H Factor: A Means of Expressing Cooking Times and Temperatures as a Single  
653       Variable. *Pulp and Paper Research Institute of Canada*, 38(2), 228–231.

654   Weise, U. (1998). Hornification - mechanisms and terminology. *Paperi Ja Puu - Paper and Timber*, 80(2), 110–  
655       115.

656   Wickholm, K., Larsson, P. T., & Iversen, T. (1998). Assignment of non-crystalline forms in cellulose I by  
657       CP/MAS <sup>13</sup>C NMR spectroscopy. *Carbohydrate Research*, 312(3), 123–129.  
658       [https://doi.org/10.1016/S0008-6215\(98\)00236-5](https://doi.org/10.1016/S0008-6215(98)00236-5)

- 659 Wollboldt, R. P., Zuckerstätter, G., Weber, H. K., Larsson, P. T., & Sixta, H. (2010). Accessibility, reactivity and  
660 supramolecular structure of E. globulus pulps with reduced xylan content. Wood Science and Technology,  
661 44(4), 533–546. <https://doi.org/10.1007/s00226-010-0370-2>
- 662 Yoon, S.-H., & van Heiningen, A. (2008). Kraft pulping and papermaking properties of hot-water pre-extracted  
663 loblolly pine in an integrated forest products biorefinery. Tappi Journal, (July), 22–27.